JOURNAL OF Applied Polymer SCIENCE

Preparation and Characterization of TiO_2 Nanofibers via Using Polylactic Acid as Template

Mengzhu Liu,[1] Zhiqiang Cheng,[1,2] Juntao Yan,[1] Linhui Qiang,[1] Xin Ru,[1] Fei Liu,[1] Dawei Ding,[1] Junfeng Li[1]

[1]College of Chemistry, Jilin University, Changchun 130012, People's Republic of China

[2]College of Resources and Environment, Jilin Agriculture University, Changchun 130118, People's Republic of China

Correspondence to: J. Li (E-mail: jfli@jlu.edu.cn)

ABSTRACT: A simple procedure is reported for the fabrication of TiO_2 nanofibers via electrospinning technique using polylactic acid (PLA), tetrabutyl titanate, and hexafluoroisopropanol as a spinning solution. TiO_2 nanofibers (600–700 nm in diameter), with bundled nanofibrils align in the fiber direction, are obtained from the calcination of the as-spun TiO_2/PLA composite nanofibers at 550°C. The structure and physicochemical property of generated nanofibers are elucidated by Fourier transform-Infrared radiation spectrometer, X-ray diffraction, scanning electron microscope, and Thermogravimetric-differential thermal analysis, respectively. The photocatalytical activity of the TiO_2 nanofibers is testified by quantifying the degradation of methylene orange. The result indicates that the TiO_2 nanofibers with pure anatase phase, which are prepared at 550°C, shows an excellent photocatalytic activity.

KEYWORDS: templates; nanofiber; catalysts; electrospinning; composites

Received 28 February 2012; accepted 4 June 2012; published online
DOI: 10.1002/app.38166

INTRODUCTION

TiO_2 has a wide variety of applications in batteries,[1] cosmetics,[2] photocatalysis,[3] hydrogen sensing,[4] solar energy conversion, and many other areas due to its possible compatibility of cost and performance.[5] The physicochemical properties of TiO_2 are different for various types of polymorphs and structures. With the development in nanotechnology, increasing attention has been paid to the study of nanoscale TiO_2 material synthesis. Lots of methods[6–8] have been used to synthesize nanocrystalline TiO_2 in the form of nanoparticles,[9] nanotubes,[10] nanowires or rods,[11] and nanofibers.[12] Among all nanophase, TiO_2 nanofibers play a key role in many applications such as biomedical materials,[9] solid-state dye-sensitized solar cells,[13] photocatalytic active layers,[14] and so on. Specially, due to their unique morphology, TiO_2 nanofibers usually exhibit higher catalytic performance compared with that of bulk TiO_2.

In recent reports, a variety of polymers such as poly(L-lysine), poly(vinyl pyrrolidone) (PVP), poly(vinyl acetate) (PVAc), b-cyclodextrin, 2,2-bis(hydroxymethyl)propionic acid, glycerin, and pentaerythritol were used as the templates to prepare nanoscale TiO_2 materials.[15–19] For these polymers, PVP and PVAc are the most commonly used polymer templates. Nuansing et al.[16] have used PVP as a template to fabricate TiO_2 nanofibers by electrospining method. Ding et al.[17] have prepared the TiO_2 nanofibers by sol-gel processing and electrospinning technique using a viscous solution of titanium iso-propoxide/PVAc. However, both PVP and PVAc templates resulted in extremely smooth TiO_2 nanofiber surfaces, which were not beneficial for enhancing the catalytic property. Many efforts have been made to discover a new template for preparing TiO_2 nanofibers with regular rougher structure.

Polylactic acid (PLA) is a highly versatile, biodegradable, aliphatic polyester derived from 100% renewable resources, such as corn and sugar beets.[20] The distribution of raw materials for PLA production is extensive. PLA does not release nitrides or sulfides during burning. On the contrary, it decomposes to give H_2O, CO_2, and humus,[20] which are beneficial to soil. PLA could combine its major advantage-degradability[21] and the control of fiber shape perfectly.[22] Furthermore, it provides excellent properties at a low price. Above all, it is obvious that PLA is a potential candidate for the preparation of nanofibers via the template route. However, PLA has been rarely used as a template to prepare nanofibers.[22,23]

Electrospinning technology is used for preparing the needed nanofibers. It is a mature method[24] to produce continuous fibers with structure of mesoporous,[25] hollow,[26] or solid.[27]

Anatase, rutile, and brookite are the three crystalline phase of TiO_2.[16] The anatase phase, which has an octahedral crystalline structure, is considered as the most efficient crystal form in photocatalytic reactions.[28] In this work, the TiO_2 nanofibers with anatase structure were obtained by electrospinning and subsequent calcinating. The solution was prepared by mixing PLA and tetrabutyl titanate (TBT) into hexafluoroisopropanol (HFIP). The composite and calcined nanofibers were elucidated by Thermogravimetric-differential thermal analysis (TG-DTA), Fourier transform-Infrared radiation (FTIR) spectrometer, X-ray diffraction (XRD), and scanning electron microscope (SEM), respectively. Comparison of the photocatalytic properties between commercial P25 and the TiO_2 nanofibers calcined at 400°C, 550°C (we called TiO_2-400 and TiO_2-550 in this article) was carried out. The results showed that the TiO_2-550 with deep striped structure exhibited excellent catalytic activity in the photoreduction reaction of methylene orange.

EXPERIMENTAL

Materials

PLA (M_w = 300,000 g/mol) was purchased from Shandong Institute of Medical Equipment. Tetrabutyl titanate (TBT, 98% chemical pure) was obtained from Huishi Biochemical Reagent (China). Hexafluoroisopropanol (HFIP, Aladdin Reagent, Shanghai, China) was used as solvents directly. Methylene orange was produced by Research Institute of Guangfu Fine Chemical Engineering in Tianjin. Commercial TiO_2 P25 came from Evonik Degussa, Germany.

Preparation of TiO_2 Nanofibers

The electrospinning solution was prepared by dissolving PLA in HFIP at a concentration of 8 wt %. When the solution became transparent after 4 h of stirring, TBT was added. The mass ratio of PLA to TBT was 3 : 4. Then, the suspension was vigorously stirred for another 4 h to get clear and pale yellow precursor gel for electrospinning. The polymer solution was loaded into a glass dropper that was connected to a high-voltage supply [DW-P303-5AC High Voltage (0–30 KV), Dongwen High-voltage Power-supply Company, China]. The voltage for electrospinning was 15 kV. A piece of flat aluminum foil was used to collect the nanofibers. The distance between the tip of the dropper and the collector was 20 cm. All electrospinning process was carried out at room temperature. The fibers were exposed to the air overnight to facilitate further hydrolyzation of TBT.

The TiO_2/PLA composite nanofibers were calcined in Muffle Furnace at 300 – 550°C for 3 h in air, with the heating rate of 10°C/min, then cooled to room temperature spontaneously.

Characterization

The pure PLA nanofibers and the as-spun composite nanofibers were subjected to TG-DTA using Pyris Diamond TG-DTA (Hengjiu Instrument, Peking, China) to compare the thermal differences and determine the temperature of possible decomposition and crystallization (or phase change) of the nanofibers. The heating rate was adjusted at 10°C/min in static air up to 900°C.

The phase structures of the as-spun TiO_2/PLA composite and calcined nanofibers were identified by XRD. The XRD measurements were performed on a Siemens D5005XRD diffractometer.

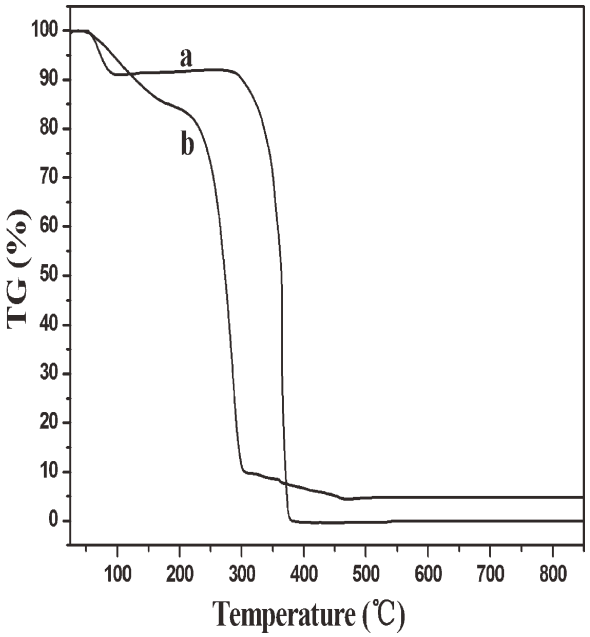

Figure 1. TG curves of (a) pure PLA nanofibers and (b) the as-spun TiO_2/PLA composite nanofibers at a heating rate of 10°C/min in static air.

The morphology and dimensions of the fibers were analyzed by SEM (SHIMDZU SSX-550, Japan). Based on the SEM images, the diameter and diameter distribution of fibers were analyzed using image visualization software ImageJ (about 100 measurements per field). In addition, FTIR spectrometer (SHIMDZU, 1.50SU1, Japan) was used to identify the vibration in functional groups present in the samples.

Photocatalytic Activity Measurement

An aqueous solution of methylene orange with the concentration of 10^{-4} mol/L was prepared. TiO_2-400 and TiO_2-550 were added into methylene orange aqueous solution with the proportion of 0.7 g/L. Each solution was added into a 10 mL vial as reactor. Then, the samples were irradiated by the ultraviolet (UV)-radiation lamp (λ = 375 nm) with continuously magnetic stirring at ambient temperature. At different intervals, a few milliliters of solution were drawn from the reaction mixture and loaded in a UV–vis spectrophotometer (SHIMDZU UV-3600, Japan). The relative concentration of methylene orange was monitored by comparing its characteristic absorption intensity of the 464 nm peak with that of the original methylene orange solution.

Under the same conditions, commercial TiO_2 P25 was used as a reference in photocatalytic degradation of methyl orange compared to TiO_2-400 and TiO_2-550 catalysts.

RESULTS AND DISCUSSION

Thermal Properties

As shown in Figure 1(a), the pure PLA nanofibers has a weight loss between 50 and 90°C. This attributes to the loss of moisture and trapped solvent (water and HFIP). After 90°C and before 290°C, the TG curve tends to be flat. And then, as the temperature continues to grow, the TG curve falls off all at a

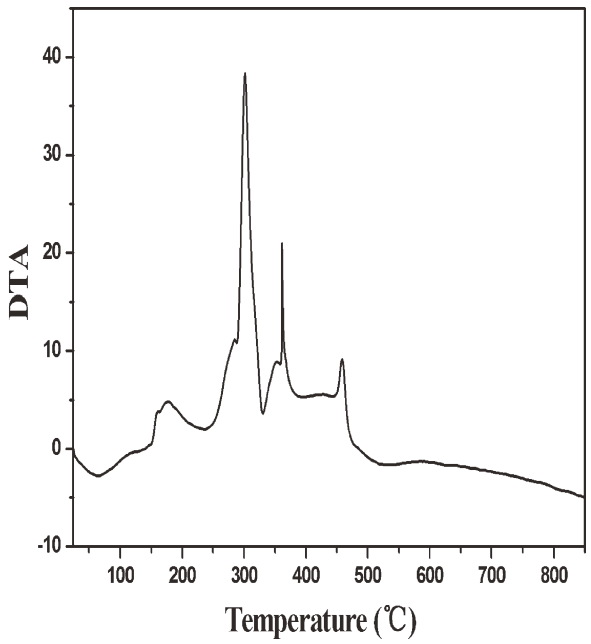

Figure 2. The DTA curve of the as-spun TiO_2/PLA composite nanofibers.

sudden. This indicates that pure PLA has decomposed under such temperature. After 400°C, no more weight loss was observed, indicating that PLA had completely decomposed at that temperature. Figure 1(b) shows the weight change of the TiO_2/PLA composite nanofibers. The TG curve goes down slowly from 60 to 220°C, which indicates the volatilization of adsorbed water and organic matter from the surface. Between 220 and 300°C, there is a significant weight loss. This is due to the decomposition of main chain of PLA. However, the TG curve of PLA [Figure 1(a)] at this corresponding temperature is flat and the temperature range in which has a dramatic decrease is 300 – 400°C. What makes such a difference is probably due to the surface structural transformation of the crystal such as physical adsorption and chemical bonding,[29] which is produced by the weak reaction between PLA and TBT. As a result, the pyrolysis temperature decreases logically. From 300 to 470°C, the TG curve goes down slowly. This owes to the formation of TiO_2 and the decomposition of few PLA which is encysted in TiO_2 crystals. At about 470°C, the TG curve is flat, whereas the DTA curve presents a small sharp exothermic peak (Figure 2), which demonstrates that there is an amorphous-anatase phase transformation. After 550°C, all of the curves were gentle. It manifests that the reaction has stopped. According to the thermogravimetric analysis, the postannealing scheme should be performed at 300, 400, and 550°C.

Structure Inspections

FTIR was used to confirm the identity of the nanofibers calcined at different temperature. As shown in Figure 3(a), the peaks at 1725, 1463, 1370, 1174, 1081 cm^{-1} are the characteristic structure of pure PLA nanofibers. Figure 3(b) depicts the spectrum of the as-spun TiO_2/PLA composite nanofibers, and it seems the same as the one shows in Figure 3(a). This indicates that TiO_2 precursor is embedded in PLA. When the nanofibers were calcined at 300°C [Figure 3(c)], the typical peaks of PLA disappeared gradually and the characteristic peaks of TiO_2 came out. This is due to the oxidation of PLA and the formation of TiO_2. As the temperature rises up, the peaks of TiO_2 exist at about 520 and 1100 cm^{-1} are more and more clear. The weak transmission band at 1650 cm^{-1} shown in Figure 3(d,e) is the H—O—H bending mode of molecularly absorbed water on the TiO_2.[30] And the corresponding peak of the stretching vibration of H—O—H appears at about 3500 cm^{-1}.

XRD patterns of the TiO_2-400 and TiO_2-550 are given in Figure 4. As shown in the picture, when the nanofibers suffered from calcinating at 400°C [Figure 4(a)], an amorphous phase was obtained. When the calcination temperature was 550°C [Figure 4(b)], the observed reflections at 2θ of 25.28, 37.76, 47.97, 53.82, and 62.70° corresponded well to the (101), (004), (200), (105), and (204) reflections of anatase phase, respectively, according to the database standard PDF 21-1272. The results of XRD patterns further confirms that the exothermic peak at 470°C in DTA curve (Figure 2) of TiO_2/PLA composite nanofibers is attributable to the crystallization of the reprecipitates transforming amorphous TiO_2 into pure anatase TiO_2 nanofibers.

Morphology and Diameter Distribution of Nanofibers

The morphology of the as-prepared TiO_2/PLA composite and calcined nanofibers is revealed by SEM shown in Figure 5. The as-spun composite nanofibers appear relatively smooth and round. Some of these nanofibers exhibit a carpenterworm-type structure, with rugged surfaces. [Figure 5(a)]. TiO_2-400 and TiO_2-550 are composed of a bundle of nanofibrils that are aligned in the fiber direction, as shown in Figure 5(b,c). This morphology of nanofibers is depicted more clearly in Figure 5(c) and is different from the previously reported TiO_2

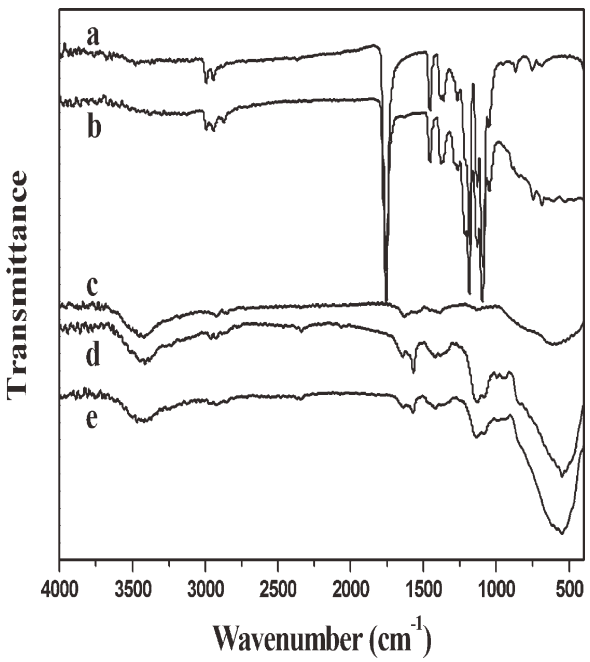

Figure 3. FTIR spectra of different samples. (a) pure PLA nanofibers; (b) as-spun TiO_2-PLA composite nanofibers; (c, d,e) are the composite nanofibers after calcination at 300, 400, and 550°C.

Applied Polymer SCIENCE

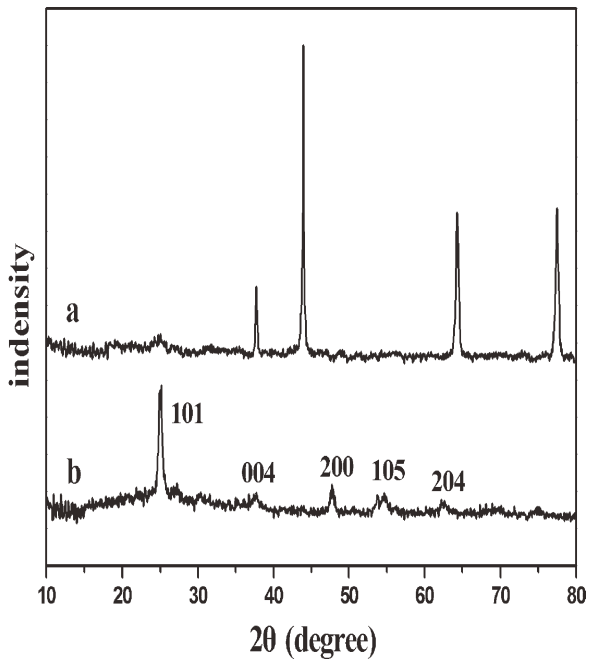

Figure 4. XRD patterns electrospun TiO_2 fibers after calcination at different temperature. (a) 400°C. (b) 550°C.

nanofibers.[31,32] This morphology indicates phase separation within the nanofibers.[33] The orientation of elongated-separated phases was formed during electrospinning and was driven by confinement and the electric field. These separated phases were converted into nanofibrils during the calcination.[12] The gap of the nanofibrils increased as the calcination temperature rose up.

Software ImageJ was used to analyze the diameter and diameter distribution of the nanofibers calcinating at different temperatures. After Gaussian fitting and statistics, the result can be seen in Figure 5. The average diameter of the as-spun PLA/TiO_2 composite nanofibers is 482 nm [Figure 6(a)], whereas the one of TiO_2-400 is 741 nm [Figure 6(b)]. It is obvious that the diameter of the calcined nanofibers has a sharp increase. This is due to the melt of PLA. When the temperature rises up to 200 –300°C, the melting PLA acts as glue and makes the nanofibers stick together. Then few PLA may be surrounded by TiO_2 crystals and most are still on the surface of the TiO_2 crystals. When the annealing temperature is above 300°C, the surface part of PLA can pyrolyze completely. The encysted part cannot thoroughly eliminate yet at this temperature, which is confirmed by TG curve. After calcination at 550°C, the average diameter of the nanofibers is decreased to 616 nm due to a complete decomposition of PLA.

Properties of Photocatalysis

The photocatalytic activities of the TiO_2 nanofibers were determined by measuring the degradation of methylene orange in an aqueous solution under UV light irradiation.

From Figure 7, it is obvious that the photocatalysis of the TiO_2-550 shows greater photocatalytic activity compared to that of TiO_2-400. The concentration changes of methylene orange under the function of TiO_2-400 is less than 5%, as shown in Figure 7(a). Whereas the concentration of methylene orange added TiO_2-550 [Figure 7(c)] changes obviously. This demonstrates that the amorphous phase of TiO_2 nearly has no photocatalysis and the anatase phase is the most useful form.

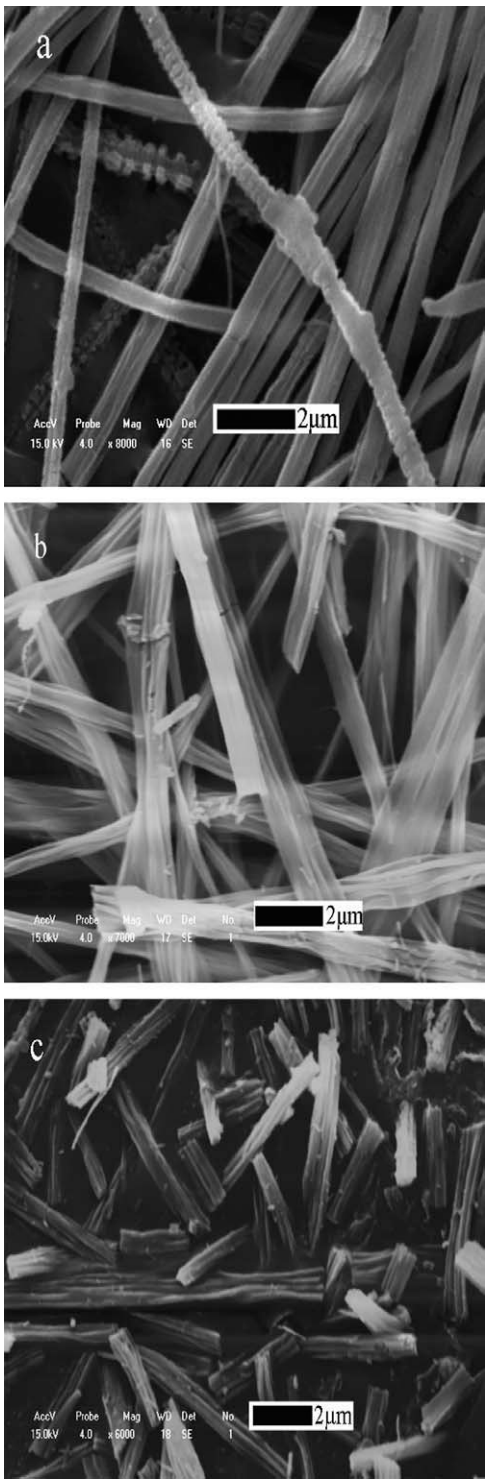

Figure 5. SEM micrograghs of different nanofibers. (a) the as-spun TiO_2/PLA composite nanofibers; (b, c) are TiO_2-400 and TiO_2-550.

Commercial TiO_2 P25 [Figure 7(b)] is used to compare the photocatalysis degradation ability with the TiO_2-550. It can be seen that the degradation rate of the methylene orange with TiO_2-550 is higher than the one with commercial P25. After irradiated under the UV light for 240 min, the concentration changes of methylene orange added TiO_2-550 and commercial P25 tended to be equal. This indicates that the TiO_2 nanofibers prepared under 550°C has an excellent photocatalytic activity.

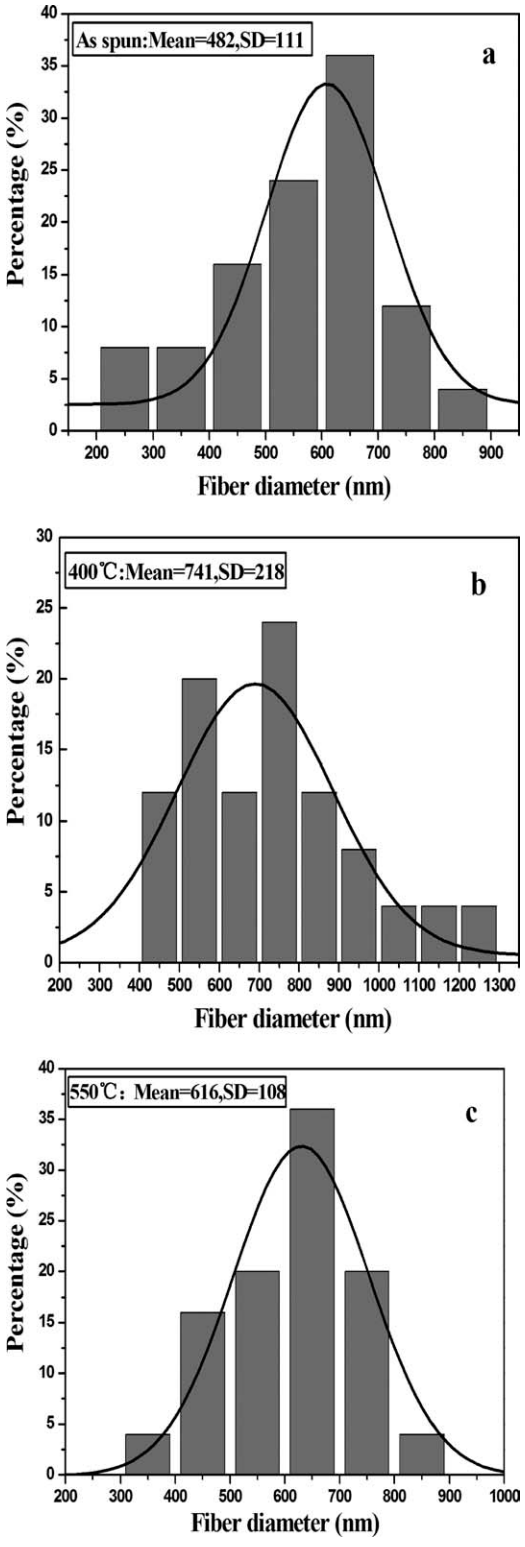

Figure 6. The size distribution of different nanofibers. (a) the as-spun TiO_2/PLA composite nanofibers; (b, c) are TiO_2-400 and TiO_2-550.

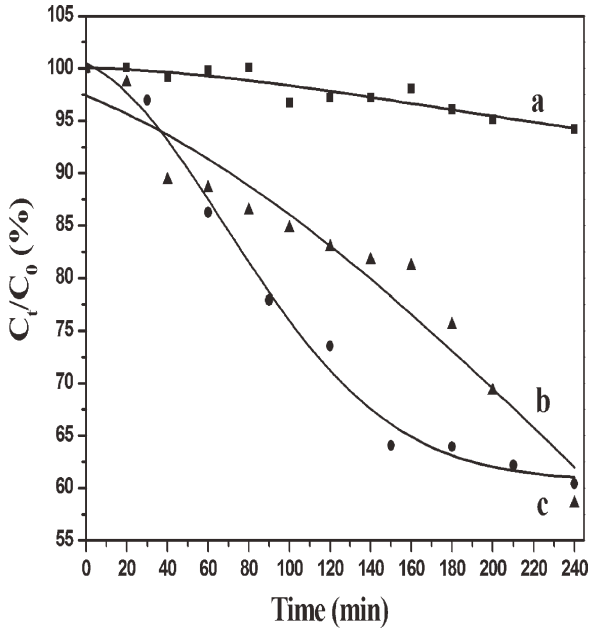

Figure 7. The methylene orange concentration changes as a function of time after added different photocatalysis. (a) TiO_2-400; (b) commercial TiO_2 P25; (c) TiO_2-550.

CONCLUSIONS

In this study, we have demonstrated PLA could be used as template to prepare pure anatase TiO_2 nanofibers with deep striped structure. The representative spin dope containing TBT as the precursor and PLA as the carrying polymer (with the TBT/PLA mass ratio being 4/3) were prepared using HFIP as the solvent. TiO_2 nanofibers with a diameter of 600 –700 nm have been prepared after calcination of the as-spun TiO_2/PLA composite nanofibers in air at 550°C for 3 h. The calcined TiO_2 nanofibers were characterized by TG, FTIR, SEM, XRD, and UV-Vis techniques. Methylene orange was used to evaluate the photocatalytic property of the resulting TiO_2. In comparison with the commercial TiO_2 Degussa P25, the anatase phase TiO_2 nanofibers (TiO_2-550) performed a similar degradation behavior, even at a faster rate. Further, these findings provide clues which lead us to believe that the TiO_2-550 should represent a promising material for photocatalytic research.

ACKNOWLEDGMENT

The authors express thanks to teacher Lianxiang Yu for her assistance with the XRD measurements.

REFERENCES

1. Wang, H. E.; Cheng, H.; Liu, C. P.; Chen, X.; Jiang, Q. L.; Lu, Z. G.; Li, Y. Y.; Chung, C. Y.; Zhang, W. J.; Zapien, J. A.; Martinu, L.; Bello, I. *J. Power Sources* **2011,** *19*, 6394.

2. Demiana, N. *J. Cosmet. Sci.* **2011,** *33*, 70.
3. Bozhidar, I. S.; Nina, V. K.; Gianluca, L. P.; Ceco, D. D. *Colloid. Surf. A* **2011,** *382*, 219.
4. Su, Z. X.; Zhou, W. Z. *J. Mater. Chem.* **2011,** *21*, 8955.
5. Tada, H.; Fujishimaa, M.; Kobayashi, H. *Chem. Soc. Rev.* **2011,** *40*, 4232.
6. Su, C.; Hong, B. Y.; Tseng, C. M. *Catal. Today.* **2004,** *96*, 119.
7. Murugan, A. V.; Samuel, V.; Ravi, V. *Mater. Lett.* **2006,** *60*, 479.
8. Zhao, B.; Chen, F.; Liu, H. Q.; Zhang, J. L. *J. Phys. Chem. Solids* **2011,** *72*, 201.
9. Faheem, A. S.; Muzafar, A. K.; Hak, Y. K.; Hern, K. *Appl. Surf. Sci.* **2010,** *257*, 296.
10. Qiu, Y. J.; Yu, J. *Solid State Commun.* **2008,** *148*, 556.
11. Limmer, S. J.; Seraji, S.; Forbess, J.; Wu, Y.; Chou, P.; Nguyen, C.; Cao, G. *Adv. Mater.* **2001,** *13*, 1269.
12. Chuangchote, S.; Jitputti, J.; Sagawa, T.; Yoshikawa, S. *ACS Appl.Mater. Inter.* **2009,** *1*, 1140.
13. Song, M. Y.; Kim, D. K.; Ihn, K. J.; Jo, S. M.; Kim, D. Y. *Synth. Met.* **2005,** *153*, 77.
14. Laera, G.; BoJin, H.; Lopez, A. *Catal. Today.* **2011,** *161*, 147.
15. Sarah, L. S.; David, W. W. *Chem. Mater.* **2006,** *18*, 3108.
16. Nuansing, W. W.; Ninmuang, S.; Jarernboon, W.; Maensiria, S.; Seraphin, S. *Mater. Sci. Eng. B.* **2006,** *131*, 147.
17. Ding, B.; Kim, C. K.; Kim, H. Y.; Seo, M. K.; Park, S. J. *Fiber. Polym.* **2004,** *5*, 105.
18. Zheng, J. Y.; Pang, J. B.; Qiu, K. Y.; Wei, Y. J. *Mater. Chem.* **2001,** *11*, 3367.
19. Zheng, J. Y.; Qiu, K. Y.; Feng, Q. W.; Xu, J. G.; Wei, Y. *Mol. Cryst. Liq. Cryst.* **2000,** *354*, 771.
20. Drumright, R. E.; Gruber, P. R.; Henton, D. E. *Adv. Mater.* **2000,** *12*, 1841.
21. Paul, M. A.; Alexandrea, M.; Philippe, D.; Henrist, C.; Rulmont, A.; Philippe, D. *Polymer* **2003,** *44*, 443.
22. Michael, B.; Hou, H.; Michael, I.; Thomas, F.; Michael, H.ellwig; Christoph, S.; Andreas, S.; Wendorff, J. H.; Andreas, G. *Adv. Mater.* **2000,** *12*, 637.
23. Hou, H.; Jun, Z.; Reuning, A.; Schaper, A.; Wendorff, J. H.; Greiner, A. *Macromolecules* **2002,** *35*, 2429.
24. Zhang, X.; Xu, S.; Han, G. *Mater. Lett.* **2009,** *63*, 1761.
25. Madhugiri, S.; Sun, B.; Smirniotis, P. G.; Ferraris, J. P.; Balkus, K. J. *Microporous Mesoporous Mater.* **2004,** *69*, 77.
26. Chang, G. Q.; Zheng, X.; Chen, R. Y.; Chen, X.; Chen, L. Q.; Chen, Z. *Acta. Phys-Chim Sin,* **2008,** *24*, 1790.
27. Dong, H. Y.; He, X. D.; Teng, Y. Y.; Song, F. Y.; Ma, W. *Int. J. Mater. Res.* **2011,** *102*, 194.
28. Chiarello, G. L.; Paola, A. D.; Palmisano, L.; Selli, E. *Photochem. Photobiol. Sci.* **2011,** *10*, 355.
29. Tang, Y. J.; Li, Y. M.; Song, J.; Pan, Z. D. *Acta. Phys-Chim. Sin.* **2007,** *23*, 717.
30. Wang, H. Q.; Wu, Z. B.; Zhao, W. R.; Guan, B. H. *Chemosphere* **2007,** *66*, 185.
31. Li, D.; Xia, Y. *Nano Lett.* **2003,** *3*, 555.
32. Song, M. Y.; Ahn, Y. R.; Jo, S. M.; Kim, D. Y. *Appl. Phys. Lett.* **2005,** *87*, DOI: 10.1063/1.2048816.
33. Chuangchote, S.; Sagawa, T.; Yoshikawa, S. *Appl. Phys. Lett.* **2008,** *93*, DOI: 10.1063/1.2958347.